THE JOURNAL OF BIOLOGICAL CHEMISTRY
Vol. 274, No. 47, Issue of November 19, pp. 33609–33615, 1999
Printed in U.S.A.

Trypanosoma cruzi Contains Major Pyrophosphate Stores, and Its Growth *in Vitro* and *in Vivo* Is Blocked by Pyrophosphate Analogs*

(Received for publication, May 25, 1999, and in revised form, September 14, 1999)

Julio A. Urbina‡§¶‖, Benjamin Moreno‡§, Stephanie Vierkotter‡§, Eric Oldfield‡§, Gilberto Payares‡‡, Cristina Sanoja‡‡, Brian N. Bailey¶, Wen Yan¶, David A. Scott¶, Silvia N. J. Moreno¶, and Roberto Docampo¶§§**

From the Departments of ‡Chemistry and §Biophysics and the ¶Laboratory of Molecular Parasitology, Department of Pathobiology, University of Illinois, Urbana-Champaign, Illinois 61802 and the ‡‡Departamento de Parasitología, Instituto de Zoología Tropical, Facultad de Ciencias, Universidad Central de Venezuela, Caracas 1040, Venezuela

High field ^{31}P nuclear magnetic resonance spectroscopy showed that inorganic pyrophosphate ($P_2O_7^{4-}$) is more abundant than ATP in *Trypanosoma cruzi*, the causative agents of Chagas' disease. These results were confirmed by specific analytical assays, which showed that in epimastigotes, the concentrations of inorganic pyrophosphate and ATP were 194.7 ± 25.9 and 37.6 ± 5.5 nmol/mg of protein, respectively, and for the amastigote form, the corresponding concentrations were 358.0 ± 17.0 and 36.0 ± 1.9 nmol/mg of protein. High performance liquid chromatographic analysis of perchloric acid extracts of epimastigotes labeled for 3 h with ^{32}P-orthophosphate showed a significant incorporation of the precursor into inorganic pyrophosphate. Inorganic pyrophosphate was not uniformly distributed in *T. cruzi* but was shown by ^{31}P-NMR and chemical analysis to be particularly associated with acidocalcisomes, organelles shown previously to contain large amounts of phosphorus and various elements. Electron microscopy analysis of pyrophosphatase-treated permeabilized epimastigotes showed disappearance of the electron density of the acidocalcisomes. Nonmetabolizable analogs of pyrophosphate, currently used for the treatment of bone resorption disorders, selectively inhibited the proliferation of intracellular *T. cruzi* amastigotes and produced a profound suppression in the number of circulating trypomastigotes in mice with an acute infection of *T. cruzi*, offering a potentially new route to chemotherapy.

Infections caused by *Trypanosoma cruzi* are among the most widespread parasitic diseases in Latin America and are responsible for heavy socioeconomic losses. There is therefore considerable interest in developing novel chemotherapeutic approaches, based on unique aspects of the structure and metabolism of this parasite. *T. cruzi* develops intracellularly in its vertebrate hosts and is confronted during its life cycle with drastic changes in its microenvironment. Survival through such complex environmental changes requires appropriate reserves of carbon and energy sources, as well as signaling species, such as Ca^{2+}. Recent work has led to the identification of an acidic calcium pool (acidocalcisome) in this organism (1–4) that contains most of its cellular Ca^{2+}, together with large amounts of magnesium, sodium, zinc, and phosphorus (3). However, the precise chemical nature of the phosphorus compound(s) in these vacuoles was not determined.

In this work, we used ^{31}P nuclear magnetic resonance (NMR) spectroscopy to investigate the nature of the acidocalcisomal phosphorus. ^{31}P NMR has been extensively used in the past to study the energy metabolism of several microorganisms, as well as that of living vertebrate tissues (5, 6). It has been particularly useful in the identification of phosphorus-based storage compounds, such as polyphosphates (7, 8), and sugar phosphates and diphosphates (9, 10). Our results indicate that pyrophosphate is more abundant than ATP in the replicating forms of the parasite and is partly located in acidocalcisomes. Together with our previous results (1–4), this shows that these organelles are unique. We also show that pyrophosphate analogs inhibit the proliferation of these parasites both *in vitro* and *in vivo*.

EXPERIMENTAL PROCEDURES

Culture Methods—Epimastigotes of *T. cruzi* Y strain or, where indicated under "Results," clone Silvio X10/4 (3) were maintained at 28 °C in BHI (1) or LIT medium (3) supplemented with 5% heat-inactivated fetal bovine serum, 100 units/ml penicillin, 100 μg/ml streptomycin, and 20 μg/ml hemin, and harvested in late exponential growth phase. The amastigote forms were cultured and purified from L_6E_9 myoblasts (1, 2). Protein was measured using the Bio-Rad Coomassie Blue method.

Preparation of Perchloric Acid Extracts and Pyrophosphatase Treatments—For NMR, *T. cruzi* epimastigotes (~2.5 g wet weight) or amastigotes (~0.5 g wet weight) were washed twice with Buffer A (116 mM NaCl, 5.4 mM KCl, 0.8 mM $MgSO_4$, 50 mM Hepes, pH 7.2, and 5.5 mM glucose) and extracted with ice-cold 0.5 M $HClO_4$ (2 ml/g of wet weight of cells). After 30 min of incubation on ice, the extracts were centrifuged at 3000 × *g* for 5 min. The supernatants were neutralized by the addition of 0.72 M KOH/0.6 M $KHCO_3$. Precipitated $KClO_4$ was removed by centrifugation at 3000 × *g* for 5 min, the supernatant separated and pH adjusted to 8.0 with 0.1 M KOH. Samples were divided into two identical portions, 2 mM $MgSO_4$ was added to each, and these were incubated in the absence or presence of inorganic pyrophosphatase (Sigma; final activity, 10 units/ml) at 30 °C, pH 7.4. Methylphosphonate was added to a final concentration of 0.1 mM as an internal NMR shift standard, and samples were made 10% (v/v) in D_2O to provide a field-frequency lock.

Electron Microscopy—For the experiments with pyrophosphatase (see Fig. 4), cells were lightly fixed with a solution of 3.5% formaldehyde in Buffer A for 5 min, washed, resuspended in Buffer A containing 2 mM

* This work was supported by National Institutes of Health Grants AI-23259 (to R. D. and S. N. J. M.) and GM-50694 and HL-19481 (to E. O.), United Nations Development Project/World Bank/World Health Organization Programme for Research and Training in Tropical Diseases Grant 970297 (to J. A. U.), and the National Research Council of Venezuela (Consejo Nacional de Investigaciones Científicas y Tecnológicas) Grant RP-IV-110034 (to G. P.). The costs of publication of this article were defrayed in part by the payment of page charges. This article must therefore be hereby marked "*advertisement*" in accordance with 18 U.S.C. Section 1734 solely to indicate this fact.

‖ A John Simon Guggenheim Foundation Fellow on leave of absence from the Instituto Venezolano de Investigaciones Científicas (Caracas, Venezuela).

** Supported by National Institutes of Health Training Grant GM-08276.

§§ To whom correspondence should be addressed: Laboratory of Molecular Parasitology, Department of Pathobiology, University of Illinois at Urbana-Champaign, 2001 S. Lincoln Ave., Urbana, IL 61802. Tel.: 217-333-3845; Fax: 217-244-7421; E-mail: rodoc@uiuc.edu.

$MgSO_4$ in the absence (control) or in the presence of 10 units/ml inorganic pyrophosphatase, and incubated for 30 min at 30 °C. Cells were washed with 0.25 M sucrose, resuspended in the same solution, applied to Formvar-coated grids for 10 min, and then blotted dry and observed directly using a Hitachi 600 electron microscope. For conventional electron microscopy (see Fig. 6), cells and fractions were treated exactly as described in Ref. 2.

^{31}P NMR Spectroscopy—^{31}P NMR spectra were obtained using a 17.625 tesla Varian INOVA NMR spectrometer, which operates at 303.6 MHz for ^{31}P (750 MHz for ^{1}H). All NMR experiments were carried out at 25 °C. Chemical shifts are reported with respect to external 85% H_3PO_4 using the convention that high frequency, low field, paramagnetic or deshielded values are positive (IUPAC convention δ-scale). Direct referencing *versus* both an external standard of 85% H_3PO_4 (replacement method) and an internal standard of methyl phosphonate (taken to be 22 ppm downfield from 85% H_3PO_4, at pH 8.0) was used.

Preparation of Cell Fractions—For Percoll subcellular fractionation, we used a previous method (4) except that a fluoride (15 mM)-containing lysis buffer was used. Other experimental details such as protocols for density gradients and enzyme assays were as described previously (3, 4).

Assays of Inorganic Pyrophosphate and ATP in Whole Cell Extracts—Pyrophosphate was determined by measuring phosphate released by inorganic pyrophosphatase using perchloric acid extracts from 0.1 g of cells (11). Nucleotides were assayed by separating perchloric acid extracts by HPLC[1] using an Isco ternary gradient system fitted with a 0.46 × 25-cm (10 μm) Partisil Sax column (Alltech) (12).

HPLC Analysis of ^{32}P-Labeled Compounds—Cells (1.2×10^8 epimastigotes/ml) were prelabeled with 5 μCi of [^{32}P]orthophosphate for 3 h in Buffer A (total volume, 60 ml) at 30 °C. At the end of the labeling period, cells were centrifuged and washed twice in 0.25 M sucrose and once in lysis buffer (20 mM Hepes, pH 7.2, 35 mM KCl, 125 mM sucrose, 5 mM dithiothreitol, 0.5 mM EDTA, 50 μg/ml DNase, 50 μg/ml RNase, 2 μM leupeptin, 2 μM *trans*-epoxysuccinyl-L-leucylamido-(4-guanidino)butane, 2 μM pepstatin, 2 μg/ml aprotinin, and 1 mM phenylmethylsulfonyl fluoride). The cell pellet was mixed with 1.5 × wet weight silicon carbide and ground with a mortar and pestle until lysis was greater than 90% (generally 40 s). Silicon carbide and unlysed cells were removed by centrifugation twice at 150 × *g* for 5 min. The supernatant was first centrifuged at 10,500 × *g* for 20 min and then at 105,000 × *g* for 60 min. Perchloric acid extracts of the fractions were prepared and HPLC fractionation carried out as described above for ATP determination. Some extracts were treated with yeast inorganic pyrophosphatase (10 units/ml) for 30 min at 30 °C prior to application to the column, to identify the pyrophosphate elution peak.

Growth Inhibition Assay—*T. cruzi* a mastigote proliferation in L_6E_9 myoblasts was measured by uracil incorporation or Giemsa staining (13). Invasion assays were performed as described (13).

In Vivo Studies—Female NMRI albino mice (20–25 g of body weight) were infected intraperitoneally with 10^4 trypomastigotes of the Y strain of *T. cruzi,* and intravenous treatment with pamidronate disodium (Aredia, 10 mg/kg/day) dissolved in sterile phosphate buffer was started 4 days postinfection; pamidronate disodium was given daily for a total of seven doses. Controls received the vehicle. Parasitemia determinations and handling of the experimental animals were carried out as described in Ref. 14.

RESULTS

Pyrophosphate Is Abundant in T. cruzi—Fig. 1*A* shows the 303.65 MHz ^{31}P NMR spectrum of a perchloric acid extract, at pH 8.0, of the epimastigote forms of *T. cruzi*, Y strain, grown axenically. The spectrum is dominated by two principal features: a resonance at 3.8 ppm, probably associated with inorganic orthophosphate, and a principal resonance at −4.2 ppm, close to the range of the resonance frequencies of terminal phosphates of nucleotide di- and triphosphates and pyrophosphate; resonances of much lower intensity were also observed in the region of α- (−9 to −13 ppm) and β-phosphates (−15 to −20 ppm) of nucleotides. This spectrum differs markedly from those of most other cell and tissue extracts (5, 6, 15), which contain prominent resonances due to the α-, β-, and γ-phosphate groups of nucleotides. In the case of *T. cruzi* epimastigotes, the integrated intensity of the dominant peak at −4.2 ppm was 10–12 times higher than the corresponding area in the α-phosphate region (−9.1 ppm) of nucleotides (six independent experiments), implying that the peak was not of nucleotide origin. The lack of a strong resonance at −22 ppm also rules out the presence of significant amounts of soluble polyphosphates in these extracts (7, 8). Very similar features were found in spectra of perchloric acid extracts of clone Silvio X10/4 epimastigotes or of epimastigotes grown in BHI medium (results not shown) and of the intracellular amastigote forms (Fig. 1*C*) obtained from infected L_6E_9 myoblasts cultured *in vitro* at 37 °C. Extraction of perchloric acid insoluble material according to published procedures (7, 8) revealed the presence of short-chain polyphosphates in quantities comparable to that of pyrophosphate (results not shown).

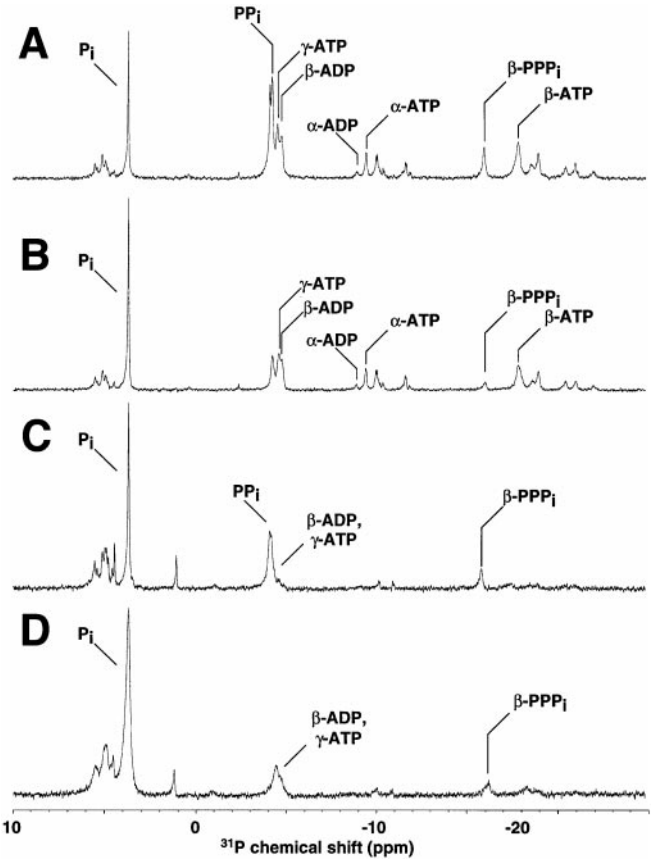

FIG. 1. **^{31}P NMR spectra of *T. cruzi*.** ^{1}H-Coupled 303.6 MHz ^{31}P NMR spectra at 25 °C of perchloric acid extracts of epimastigotes (*A* and *B*) or amastigotes (*C* and *D*) incubated in the absence (*A* and *C*) or presence (*B* and *D*) of inorganic pyrophosphatase (10 units/ml) for 60 min. Note the disappearance of the resonances at −4.2 ppm (pyrophosphate) and the increase in the intensity of the resonances at 3.8 ppm (orthophosphate). Spectra were acquired by using 1280–2560 45° pulses (14.5 μs), 32,000 data points per spectrum, a recycle delay of 1.5 s, and 3 Hz line broadening.

The origin of each of the dominant resonances present in the perchloric acid extracts was then further investigated by recording a ^{31}P-^{31}P COSY spectrum (Fig. 2). This showed that the −4.2 ppm resonance was not correlated with any others in the two-dimensional spectrum and that the less intense resonances at −4.54 and −4.85 ppm were correlated only with resonances in the β-phosphate region (−16.2 and −18.2 ppm), whereas a much smaller resonance at −5.21 ppm had correlations with both α- and β-phosphate resonances (−9.1 and −19.3 ppm). These results imply that the dominant resonance at −4.2 ppm is due to pyrophosphate, whereas those at −4.54, −4.85, and −5.21 ppm can be tentatively assigned to the terminal phos-

[1] The abbreviation used is: HPLC, high performance liquid chromatography.

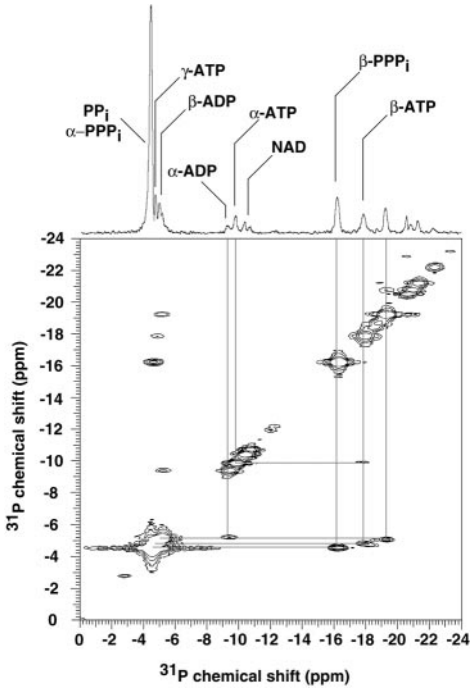

FIG. 2. **Two-dimensional COSY ^{31}P NMR spectrum of a perchloric acid extract of *T. cruzi* epimastigotes.** The COSY spectrum was acquired with 90° pulses (25 μs), in the presence of ^{1}H WALTZ decoupling with 128 steps in the F1 dimension (800 scans each). The spectrum was zero-filled to 2048 in the F1 and 4096 data points in the F2 dimension. Both sine-bell (0.067 s) and exponential (30 Hz broadening) apodizations were applied in the F2 domain, whereas only a sine bell (0.004 s) was applied in F1, prior to Fourier transformation, and the total acquisition time was 42.8 h.

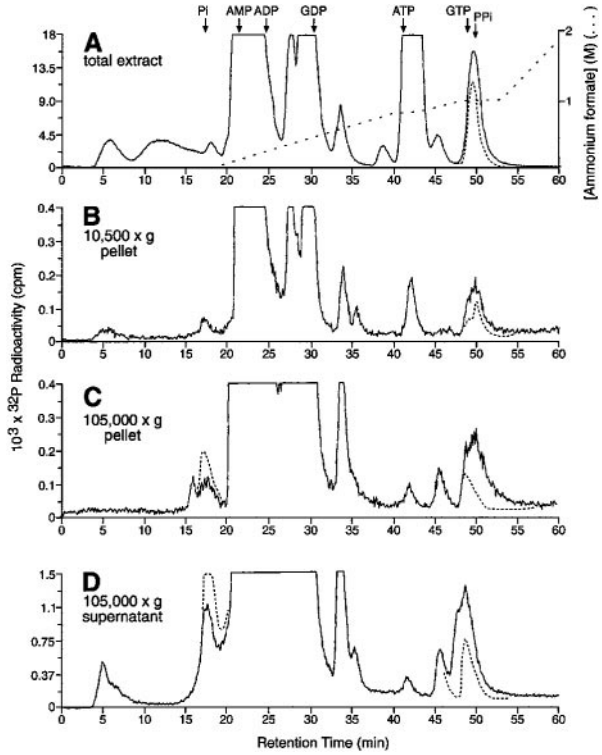

FIG. 3. **Distribution and ^{32}P labeling of phosphorylated compounds in subcellular fractions of *T. cruzi* epimastigotes.** Cells (1.2 × 10^8 epimastigotes/ml) were prelabeled with 5 μCi of [^{32}P]orthophosphate for 3 h in Buffer A at 30 °C. At the end of the labeling period, the cells were washed three times in Dulbecco's phosphate-buffered saline. Whole cells or subcellular fractions were obtained, perchloric acid extracts prepared, and HPLC fractionation carried out as described under "Experimental Procedures." *A,* whole epimastigote extracts; *B,* 10,500 × *g* for 20 min pellet; *C,* 105,000 × *g* for 60 min pellet; and *D,* 105,000 × *g* for 60 min supernatant. The extracts were treated (*dashed lines*) or not (*solid lines*) with yeast inorganic pyrophosphatase (10 units/ml) for 30 min at 30 °C, prior to application to the column. Note the decreased ^{32}P label in the *PPi* region and an increase in the level of inorganic orthophosphate (P_i), most evident in the 105,000 × *g* pellet (*C*) and supernatant (*D*).

phate groups of triphosphate, tetraphosphate, and the γ-phosphate of nucleoside triphosphates, respectively. The assignment of the −4.2 ppm resonance to pyrophosphate was then substantiated by "spiking" the samples with pure $Na_2P_2O_7$, which resulted in an increase in intensity of this resonance (not shown). Additional support for these assignments was then also obtained by incubating the perchloric acid extracts with pure yeast inorganic pyrophosphatase. After 60 min of treatment of the extracts of epimastigotes (Fig. 1*B*) or amastigotes (Fig. 1*D*), the resonances at −4.2 ppm were reduced, and there were concomitant stoichiometric increases in the intensity of the resonances at 3.8 ppm assigned to inorganic orthophosphate (Fig. 1, *B* and *D*). The presence of pyrophosphate was also confirmed by enzymatic assay using yeast pyrophosphatase. This gave a pyrophosphate concentration of 194.7 ± 25.9 nmol/mg of protein for epimastigotes and 358 ± 17 nmol/mg of protein (n = 3) for amastigotes of *T. cruzi*, values that were much higher than the concentrations of ATP in the same extracts (37.6 ± 5.5 and 36.0 ± 1.9 nmol/mg of protein, respectively; n = 3), as assayed by HPLC. Taken together, these results indicate that pyrophosphate is more abundant than ATP in *T. cruzi*.

Low Pyrophosphate Turnover in Epimastigotes—HPLC analysis of ^{32}P-labeled compounds in perchloric acid extracts of cells labeled during a 3-h incubation with [^{32}P]orthophosphate also indicated the presence of a significant inorganic pyrophosphate component (which co-eluted with GTP; Fig. 3*A, solid line*), identified by comparison with an authentic standard and by its decrease after incubation with inorganic pyrophosphatase (Fig. 3*A, dashed line*). After this labeling period, most of the labeled phosphorus was detected in nucleotides (ATP, ADP, AMP, GTP, and GDP) and only 2.2 ± 0.2% (n = 4) of the total radioactivity incorporated was detected as pyrophosphate, indicating relatively low metabolic turnover.

Subcellular Localization of Pyrophosphate in T. cruzi—When subcellular fractions of epimastigotes prelabeled for 3 h with ^{32}P were analyzed (Fig. 3, *B–D*), labeling of pyrophosphate was more noticeable in the supernatant fraction (78% of the total pyrophosphate identified) than in the 10,500 × *g* (5.1%) or 105,000 × *g* (16%) pellets. The amount of radioactivity with an elution time corresponding to [^{32}P]pyrophosphate decreased and that corresponding to [^{32}P]orthophosphate increased significantly after incubation of the extracts from the supernatant and 105,000 × *g* pellet fractions with inorganic pyrophosphatase, whereas a smaller decrease was detected in the extract of the 10,500 × *g* pellet (Fig. 3, *dashed line*), suggesting a lower turnover of the compound in this fraction, which contains acidocalcisomes and mitochondria. As a control for breakage of acidocalcisomes during cell lysis, we measured zinc levels in each fraction by using atomic absorption spectroscopy. Zinc was shown previously to be accumulated in the acidocalcisomal matrix, but not elsewhere in *T. cruzi* epimastigotes (3). Of a total of 700 μg of zinc detected, 92% was found in the 10,500 × *g* pellet fraction, 2% in the 105,000 × *g* pellet fraction, and 6% in the 105,000 × *g* supernatant fraction (whereas the protein distribution was 36, 23, and 41%, respectively, of 80 mg of protein total). This indicated that little of the acidocalcisome matrix was released into the soluble fraction during cell lysis.

In previous work (3), we have shown by electron microscopy

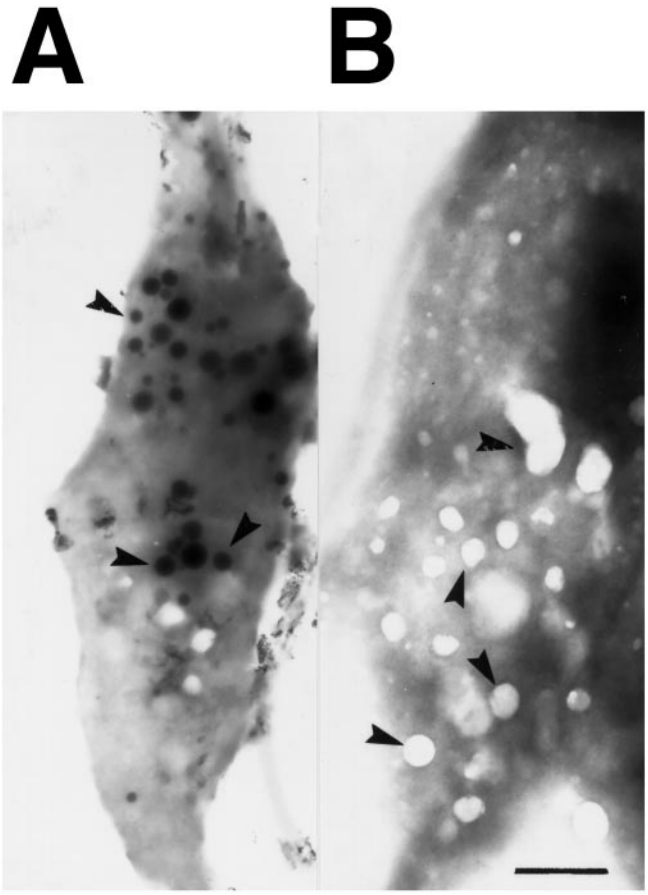

FIG. 4. **Ultrastructure of unstained epimastigotes.** *Arrowheads* show acidocalcisomes (*A*) or the empty vacuoles that are left after pyrophosphatase treatment (*B*); *bar,* 1 μm.

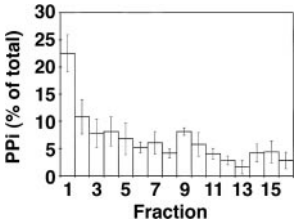

FIG. 5. **Distribution of pyrophosphate on Percoll density gradients of *T. cruzi* epimastigote homogenates.** Results are the mean ± S.E. of four different experiments. Fraction 1 is at the bottom of the gradient.

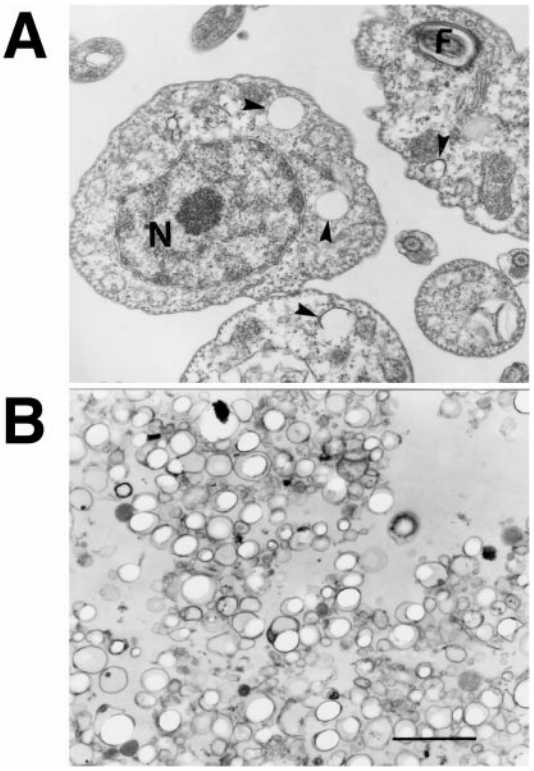

FIG. 6. **Conventional electron micrographs of whole *T. cruzi* epimastigotes (*A*) and isolated acidocalcisomes (*B*); *bar*, 1 μm.**

techniques that acidocalcisomes correspond to the electron-dense vacuoles observed in whole, unstained epimastigotes and contain large amounts of phosphorus. To investigate whether pyrophosphate was present in acidocalcisomes, we treated intact epimastigotes with formaldehyde (to permeabilize their plasma membrane), followed by incubation for 30 min with yeast inorganic pyrophosphatase. This treatment resulted in complete loss of the electron density of the acidocalcisomes (Fig. 4), suggesting that pyrophosphate (complexed with cations) was the main electron dense material of these organelles. No changes were observed in control cells exposed to the same treatment without pyrophosphatase (Fig. 4*A*).

To confirm the presence of pyrophosphate in acidocalcisomes, these organelles were separated on Percoll gradients as described previously (4) and analyzed for the presence of pyrophosphate both enzymatically and by ^{31}P NMR. The fractionation procedure was carried out in the presence of 15 mM potassium fluoride to inhibit endogenous pyrophosphatase activity (4). The densest fraction (fraction 1) from the Percoll gradients contained a significant amount (23% of the total pyrophosphate recovered) of cellular pyrophosphate (Fig. 5), which correlated well with the distribution of proton-translocating pyrophosphatase activity, an acidocalcisomal marker (4). Standard transmission electron microscopy of the densest fraction showed that it contained organelles similar to the acidocalcisomes seen in intact cells (Fig. 6) (3). The ^{31}P NMR spectrum of combined fractions 1–3 (Fig. 7*A*) contains a resonance at −0.8 ppm, attributed to pyrophosphate in the acidic environment of acidocalcisomes, plus a resonance at −5.4 ppm, which is the expected chemical shift of free pyrophosphate at the pH (8.0) of the experiment. Two peaks attributable to orthophosphate at 2.4 and 2.5 ppm were also detected. This suggested that resonances from both pyrophosphate and orthophosphate inside and outside acidocalcisomes were being detected. On addition of 0.1% Triton X-100 (to disrupt the acidocalcisomal membrane), and in the presence of KF to inhibit the acidocalcisomal pyrophosphatase (4), there was a large increase in the intensity of the −5.4 ppm peak, due to pyrophosphate release from most acidocalcisomes (Fig. 7*B*), whereas the two orthophosphate resonances collapsed to a single peak at −5.4 ppm. Notably, in the absence of KF (Fig. 7*C*), there was no detectable peak at −5.4 ppm, which can be attributed to the rapid hydrolysis of inorganic pyrophosphate to phosphate. Thus, these ^{31}P NMR results strongly support the idea that a significant amount of pyrophosphate is located in the acidocalcisomes. However, both the [^{32}P]orthophosphate-labeling experiments (Fig. 3) and the fractionation studies (Fig. 5) suggest the presence of a significant amount of pyrophosphate in other compartments, including the cytosolic fraction, contributing to the overall high PPi level.

Pyrophosphate Analogs Selectively Block the Intracellular Proliferation of T. cruzi—The observation that pyrophosphate is one of the most abundant phosphorylated compound in *T. cruzi,* together with the recent discovery of several pyrophosphate-utilizing enzymes in these parasites (4, 16), suggests

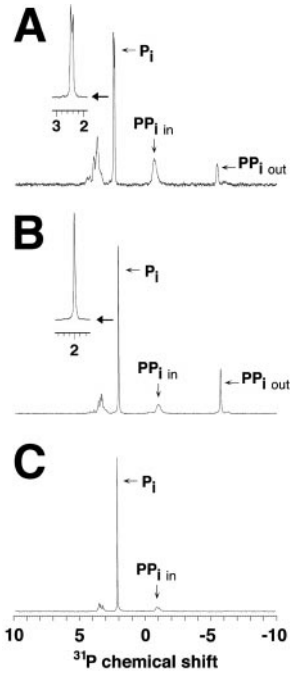

FIG. 7. **^{31}P NMR spectra of acidocalcisomes.** ^{31}P NMR spectra of acidocalcisomal fractions of *T. cruzi* epimastigotes taken directly from Percoll gradients and adjusted to pH 8.0. *A,* ^{1}H-Coupled 303.6 MHz ^{31}P NMR spectra of Percoll gradient fractions 1–3, in the presence of 15 mM sodium fluoride; *B,* 15 mM sodium fluoride plus 0.1% (v/v) Triton X-100; *C,* 0.1% (v/v) Triton X-100, without sodium fluoride. 1280 scans were accumulated, using 45° pulse (14.5 μs) excitation, a 1.5-s recycle delay, and 3 Hz line broadening, prior to Fourier transformation. PPi_{in} and PPi_{out} indicate the peaks attributed to pyrophosphate inside and outside the acidocalcisomes, respectively. The *insets* show the changes in the orthophosphate resonance.

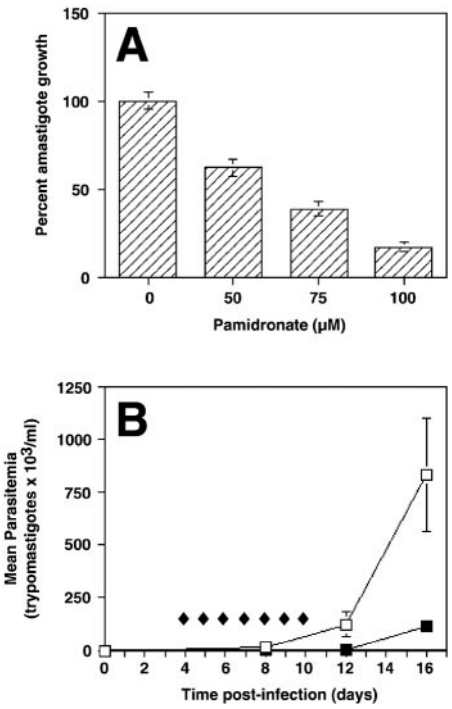

FIG. 8. **Effects of pamidronate on the intracellular proliferation of *T. cruzi* amastigotes *in vitro* (*A*) and in a murine model of acute Chagas' disease (*B*).** *A,* amastigote growth was quantified by measuring [^{3}H]uracil incorporation after 70 h of infection. *B,* pamidronate (10 mg/kg/day) or control vehicle was given daily for a total of seven doses (*diamonds*). There were statistically significant differences in the parasitemias of control (*open squares*) and treated (*closed squares*) animals at all time points ($p < 0.05$; Student's t test; $n = 6$).

that this compound could have essential roles in the metabolism of these parasites and that pyrophosphate-utilizing enzymes might serve as new drug targets. The *T. cruzi* acidocalcisomal pyrophosphatase was inhibited *in vitro* (4) by a nonmetabolizable pyrophosphate analog, 2-aminoethylene-1,1-bisphosphonate, as seen previously with the *Vigna radiata* enzyme (17). This suggested that bisphosphonate derivatives might interfere with parasite growth. To test this idea, we monitored the growth of *T. cruzi* amastigotes in L_6E_9 myoblasts in the presence of different concentrations of the bisphosphonate pamidronate (3-amino-1-hydroxypropylidene)bisphosphonate), a bisphosphonate currently used clinically in the treatment of bone resorption disorders (18). Results are shown in Fig. 8*A*. Amastigote proliferation, as assayed by uracil incorporation, was significantly inhibited, with a 50% inhibition at about 65 μM pamidronate. [^{3}H]Uracil incorporation in the presence of different concentrations of pamidronate correlated closely with the number of parasites per 100 host cells in Giemsa-stained monolayers under the conditions used. The linear correlation coefficient for the data was 0.991 (data not shown). No toxicity to the host cells, as assessed by phase contrast microscopy observation of detachment, vacuolation, and rounding of the cells, was detected except at high concentrations of bisphosphonates (>300 μM), as reported before (19). Invasion of host cells by the parasite was not affected by this compound. Other bisphosphonates were also effective in inhibiting intracellular proliferation of *T. cruzi*. Alendronate (4-amino-1-hydroxybutylidene)bisphosphonate) was as effective as pamidronate against this parasite (IC_{50} = 65 μM), whereas risedronate (1-hydroxy-2-(3-pyridinyl)-ethylidene)bisphosphonate) was less effective (IC_{50} = ~300 μM). When tested on the vacuolar acidocalcisomal pyrophosphatase activity, the inhibitory concentrations were higher (IC_{50} = 256 and 90 μM for alendronate and pamidronate, respectively, whereas 500 μM risedronate inhibited the pyrophosphatase activity by only 25%).

Pamidronate Blocks the Intracellular Proliferation of T. cruzi in Vivo—We also tested the activity of pamidronate in a murine model of acute Chagas' disease (14). Pamidronate given intravenously to mice with an acute *T. cruzi* infection completely arrested the development of parasitemia during treatment (Fig. 8*B*); parasitemia levels remained at <3 and <15% of those in control animals 2 and 6 days after the end of treatment, respectively. This experiment, designed as a proof of concept, clearly demonstrates that pamidronate can effectively suppress the proliferation of the parasite *in vivo*, in accord with its *in vitro* effects (Fig. 8).

DISCUSSION

In this work, we have shown that inorganic pyrophosphate is more abundant than ATP in the proliferative stages of *T. cruzi* and is located in part (around 23% of the total) in acidocalcisomes. Previous studies of *T. cruzi* using subcellular fractionation, gold-labeled transferrin, and molecular biological techniques have provided evidence that acidocalcisomes are different from lysosomes and other components of the endocytic pathway in these parasites (1–4). The present results further support the hypothesis that acidocalcisomes are organelles with their own unique set of characteristics. Acidocalcisomes are also present in other trypanosomatids, such as *Trypanosoma brucei* (20–22) and *Leishmania amazonensis* (23), and in apicomplexan parasites, such as *Toxoplasma gondii* (24), and we have confirmed than in most of these organisms, pyrophosphate is more abundant than ATP.[2]

[2] J. A. Urbina, B. Moreno, E. Oldfield, B. N. Bailey, D. A. Scott,

The presence of pyrophosphate in "volutin" granules (vacuoles stained pink with basic blue dyes), which are also rich in calcium and magnesium, has been described in the free-living ciliate *Tetrahymena pyriformis* by direct chemical analysis (25, 26) and ^{31}P NMR (27). The dense granules of blood platelets are also known to contain pyrophosphate together with ATP, ADP, and serotonin (28). Previous studies in trypanosomatids have demonstrated the presence of a high concentration of pyrophosphate in *Leishmania major* (11), although its subcellular localization was not established.

Inorganic pyrophosphate was for a long time believed to be merely a byproduct of biosynthetic reactions (synthesis of nucleic acids, coenzymes, proteins, activation of fatty acids, and isoprenoid synthesis) subject to immediate hydrolysis by inorganic pyrophosphatases. From the early 1960s, however, data have accumulated suggesting an important bioenergetic and regulatory role for this compound (29). Pyrophosphate-dependent enzymes have been found in plants, animal tissues, and microorganisms. Pyrophosphate biosynthesis, coupled to the respiratory chain, was described for yeast, animal, and plant mitochondria (29). In plants (30) and in some parasitic protozoa, pyrophosphate is used in place of ATP as an energy donor in several reactions, such as the pyrophosphate-phosphofructokinase of *Trichomonas vaginalis* (31), *Entamoeba histolytica* (32), *Giardia lamblia* (33), *Naegleria fowleri* (34), *T. gondii* (35, 36), *Cryptosporidium parvum* (36), and *Eimeria tenella* (36); the pyruvate, phosphate dikinase of *Giardia lamblia* (37), *Entamoeba histolytica* (38), and trypanosomatids (16); or the phosphoenolpyruvate carboxytransphosphorylase (39) and the pyrophosphate-acetate kinase (40) of *E. histolytica*. It has been postulated that pyrophosphate analogs could be selective inhibitors of some of these parasite enzymes (41). In addition, we recently detected a proton-translocating pyrophosphatase activity located in acidocalcisomes of *T. cruzi* (4), which is inhibited by a bisphosphonate derivative, in a fashion similar to the plant enzyme (17). As the acidity of the acidocalcisomal lumen seems to be required for Ca^{2+} accumulation (1), these results suggest that pyrophosphate plays a crucial role in the survival of the parasite. Interestingly, a pyrophosphatase activity was also suggested to be associated in membrane-like structures surrounding the pyrophosphate-rich granules of *T. pyriformis* (25, 26).

Although some of the pyrophosphate analogs (bisphosphonates) tested were effective in inhibiting *T. cruzi* growth *in vitro* and *in vivo*, correlation between their growth inhibitory concentrations and inhibition of the acidocalcisomal V-H^+-PPase activity was limited. This suggests that these drugs may be acting against other cellular processes possibly involve pyrophosphate. Given the bisphosphonate structure, these molecules are putative inhibitors of intracellular pathways involving phosphate or pyrophosphate. Bisphosphonates suppress osteoclastic bone resorption and are used extensively in the treatment of common skeletal disorders, such as osteoporosis, metastatic bone disease, and Paget's disease of bone (18, 42). The intracellular targets of bisphosphonates have not yet been identified. However, structure-activity relationship investigations of bone resorption inhibition, slime mold cell growth, and macrophage apoptosis support the assumption that nitrogen-containing bisphosphonates interact with a highly specific target inside the cells (42). Some bisphosphonates, such as clodronate, can be metabolized to a cytotoxic, nonhydrolyzable analog of ATP by mammalian cells (43), and one inhibits the osteoclast vacuolar H^+-ATPase (44). However, the more potent nitrogen-containing bisphosphonates, such as pamidronate, alendronate, ibandronate, and risedronate, are not metabolized (43) and probably act by a different mechanism that can lead to osteoclast apoptosis (45). Two potent nitrogen-containing bisphosphonates that cause apoptosis in J774 cells, YM175 and ibandronate (46), have been reported to be inhibitors of sterol biosynthesis in J774 cells (47, 48). The pathway of sterol biosynthesis from mevalonate includes the synthesis by prenyl transferases of isoprenyl-pyrophosphate intermediates, such as farnesyl pyrophosphate and geranylgeranyl pyrophosphate. These isoprenyl groups can be transferred to a cysteine residue within carboxyl-terminal motifs present in several classes of proteins, including the family of GTP-binding Ras, Rho, Rac, and Rab proteins and nuclear lamins (49, 50) in a reaction catalyzed by at least three distinct cytoplasmic prenyl protein transferases (50). Posttranslational modification of proteins with C15 farnesyl or C20 geranylgeranyl groups appears to be essential for the localization of these proteins to membranes and hence their biological function (49, 50). Inhibition of protein prenylation by substrate inhibitors of prenyl protein transferases or by inhibitors of mevalonate or isopentenyl pyrophosphate synthesis (such as lovastatin, mevastin, and phenylacetate) can lead to induction of apoptotic cell death (51). It has been shown that apoptosis induced by bisphosphonates in J774 macrophages is associated with the inhibition of post-translational prenylation of proteins, such as Ras, and that this effect can be inhibited by the addition of components of the mevalonate pathway, such as farnesyl pyrophosphate, and geranylgeranyl pyrophosphate (52). Recent studies have shown that protein prenylation occurs in *T. cruzi* and that the growth of intracellular forms of *T. cruzi* is sensitive to protein farnesyl transferase inhibitors (53). Some of the inhibitors used in these studies were monophosphonates (53). In addition, apoptosis has been found to occur in *T. cruzi* (54).

Although there may be several actual bisphosphonate target molecules, their selective anti-*T. cruzi* activity (Fig. 8) could result from their preferential accumulation in the parasite due to the presence of the calcium- and pyrophosphate-rich acidocalcisomes. A similar explanation has been advanced for the anti-osteoclastic activity of these compounds, as they are mostly accumulated in mineralized bone tissue (18). In addition, it is particularly encouraging to note that macrophages (one of the preferred host cells for *T. cruzi*), like osteoclasts, appear to be particularly susceptible to bisphosphonates, which makes them potentially useful as antiarthritic drugs (18). In addition, the concentrations of bisphosphonates used in this work are actually lower than those reached in normal tissues susceptible to infection by *T. cruzi* following established pharmacological doses. For example, in liver and spleen, pamidronate levels may reach concentrations 140 and 814 times higher than in plasma (55), and the plasma concentrations of pamidronate achieved in humans after a single intravenous administration is already around 10 μM (56). Given that large numbers of bisphosphonates are already approved for long term use in treating various bone-resorption disorders, it seems likely that such drugs will play a role in trypanosomatid chemotherapy in the future, alone or in combination with other parasite-specific therapies.

Acknowledgments—We thank Elizabeth Ujhelyi for help with the electron microscopy and Linda Brown for technical assistance. Solution NMR spectra were obtained in the Varian-Oxford Instrument Center for Excellence in NMR Laboratory. Funding for this instrumentation was provided in part from the W. M. Keck Foundation, the National Institutes of Health (RR 10444), and the National Science Foundation (CHE 96-10502).

S. N. J. Moreno, and R. Docampo, unpublished results.

REFERENCES

1. Docampo, R., Scott, D. A., Vercesi, A. E., and Moreno, S. N. J. (1995) *Biochem. J.* **310,** 1005–1012

2. Lu, H.-G., Zhong, L., de Souza, W., Benchimol, M., Moreno, S. N. J., and Docampo, R. (1998) *Mol. Cell. Biol.* **18,** 2309–2323
3. Scott, D. A., Docampo, R., Dvorak, J. A., Shi, S., and Leapman, R. (1997) *J. Biol. Chem.* **272,** 28020–28029
4. Scott, D. A., de Souza, W., Benchimol, M., Zhong, L., Lu, H.-G., Moreno, S. N. J., and Docampo, R. (1998) *J. Biol. Chem.* **273,** 22151–22158
5. Hoult, D. I., Busby, S. J. W., Gadian, D. G., Radda, G. K., Richards, R. E., and Seeley, P. J. (1974) *Nature* **252,** 285–287
6. Cerdan, S., and Seelig, J. (1990) *Annu. Rev. Biophys. Biophys. Chem.* **19,** 43–67
7. Sianoudis, J., Küsel, A. C., Mayer, A., Grimme, L. H., and Leibfritz, D. (1986) *Arch. Microbiol.* **144,** 48–54
8. Martin, J. B., Foray, M. F., Klein, G., and Satre, M. (1987) *Biochim. Biophys. Acta* **931,** 16–25
9. Hensgens, C. M. H., Santos, H., Zhang, C., Kruizinga, W. H., and Hansen, T. A. (1996) *Eur. J. Biochem.* **242,** 327–331
10. Stephens, L., Radenberg, T., Thiel, U., Vogel, G., Khoo, K.-H., Dell, A., Jackson, T. R., Hawkins, P. T., and Mayr, G. W. (1993) *J. Biol. Chem.* **268,** 4009–4015
11. Blum, J. J. (1989) *J. Protozool.* **36,** 254–257
12. Docampo, R., Gadelha, F. R., Moreno, S. N. J., Benaim, G., Hoffmann, M. E., and Vercesi, A. E. (1993) *J. Eukaryot. Microbiol.* **40,** 311–316
13. Yan, W., and Moreno, S. N. J. (1998) *J. Immunol. Methods* **220,** 123–128
14. Urbina, J. A., Payares, G., Molina, J., Sanoja, C., Liendo, A., Lazardi, K., Piras, M. M., Piras, R., Perez, N., Wincker, P., and Ryley, J. F. (1996) *Science* **273,** 969–971
15. Murphy, E. J., Brindle, K. M., Rorison, C. J., Dixon, R. M., Rajagopalan, B., and Radda, G. K. (1992) *Biochim. Biophys. Acta* **1135,** 27–34
16. Bringaud, F. Baltz, F. D., and Baltz, T. (1998) *Proc. Natl. Acad. Sci. U. S. A.* **95,** 7963–7968
17. Zhen, R.-G., Baykov, A. A., Bakuleva, N. P., and Rea, P. A. (1994) *Plant Physiol.* **104,** 153–159
18. Rogers, M. J., Watts, D. J., and Russell, R. G. G. (1997) *Cancer* **80,** 1652–1660
19. Cecchini, M. G., and Fleisch, H. (1990) *J. Bone Miner. Res.* **5,** 1019–1027
20. Vercesi, A. E., Moreno, S. N. J., and Docampo, R. (1994) *Biochem. J.* **304,** 227–233
21. Vercesi, A. E., and Docampo, R. (1996) *Biochem. J.* **315,** 265–270
22. Vercesi, A. E., Grijalba, M. T., and Docampo, R. (1997) *Biochem. J.* **328,** 479–482
23. Lu, H.-G., Zhong, L., Chang, K.-P., and Docampo, R. (1997) *J. Biol. Chem.* **272,** 9464–9473
24. Moreno, S. N. J., and Zhong, L. (1996) *Biochem. J.* **313,** 655–659
25. Rosenberg, J. (1966) *Exp. Cell Res.* **41,** 397–410
26. Rosenberg, J., and Munk, N. (1969) *Biochim. Biophys. Acta* **184,** 191–197
27. Deslauriers, R., Ekiel, I., Byrd, A., Jarrell, H. C., and Smith, I. C. P. (1982) *Biochim. Biophys. Acta* **720,** 329–337
28. Ugurbil, K., Holmsen, H., and Shulman, R. G. (1979) *Proc. Natl. Acad. Sci. U. S. A.* **76,** 2227–2231
29. Mansurova, S. E. (1989) *Biochim. Biophys. Acta* **977,** 237–247
30. Stitt, M. (1990) *Annu. Rev. Plant Physiol.* **41,** 153–185
31. Mertens, E., Van Schaftingen, E., and Müller, M. (1989) *Mol. Biochem. Parasitol.* **37,** 183–190
32. Reeves, R. E., Serrano, R., and South, D. J. (1976) *J. Biol. Chem.* **251,** 2958–2962
33. Mertens, E. (1990) *Mol. Biochem. Parasitol.* **40,** 147–150
34. Mertens, E., De Jonckheere, J., and Van Schaftingen, E. (1993) *Biochem. J.* **292,** 797–803
35. Peng, Z.-Y., and Mansour, T. E. (1992) *Mol. Biochem. Parasitol.* **54,** 223–230
36. Denton, H., Brown, S. M. A., Roberts, C. W., Alexander, J., McDonald, V., Thong, K.-W., and Coombs, G. H. (1996) *Mol. Biochem. Parasitol.* **76,** 23–29
37. Hrdy, I., Mertens, E., and Nohynkova, E. (1993) *Exp. Parasitol.* **76,** 438–441
38. Reeves, R. E., Menzies, R. A., and Hsu, D.-S. (1968) *J. Biol. Chem.* **243,** 5486–5491
39. Reeves, R. E. (1970) *Biochim. Biophys. Acta* **220,** 346–349
40. Reeves, R. E., and Guthrie, J. D. (1975) *Biochem. Biophys. Res. Commun.* **66,** 1389–1392
41. Peng, Z.-Y., Mansour, J. M., Araujo, F., Ju, J.-K., McKenna, C. E., and Mansour, T. E. (1995) *Biochem. Pharmacol.* **49,** 105–113
42. Rodan, G. A. (1998) *Annu. Rev. Pharmcol. Toxicol.* **38,** 375–388
43. Frith, J. C., Mšnkkonen, J., Balckburn, G. M., Russell, R. G. G., and Rogers, M. J. (1997) *J. Bone Miner. Res.* **12,** 1358–1367
44. David, P., Nguyan, H., Barbier, A., and Baron, R. (1996) *J. Bone Miner. Res.* **11,** 1498–1507
45. Hughers, D. E., Wright, K. R., Uy, H. L., Sasaki, A., Yoneda, T., Roodman, G. D., Mundy, G. R., and Boyce, B. F. (1995) *J. Bone Miner. Res.* **10,** 1478–1487
46. Rogers, M. J., Chilton, K. M., Coxon, F., Lawry, J., Smith, M. O., Suri, S., and Russell, R. G. G. (1996) *J. Bone Miner. Res.* **11,** 1482–1491
47. Amin, D., Cornell, S. A., Gustafson, S. K., Needle, S. J., Ulrich, J. W., Bilder, G. E., and Perrone, M. H. (1992) *J. Lipid Res.* **33,** 1657–1663
48. Amin, D., Cornell, S. A., Perrone, M. H., and Bilder, G. E (1996) *Drug. Res.* **46,** 759–762
49. Maltese, W. A. (1990) *FASEB J.* **4,** 3319–3327
50. Zhang, F. L., and Casey, P. J. (1996) *Annu. Rev. Biochem.* **65,** 241–269
51. Perez-Sala, D., and Mollinedo, F. (1994) *Biochem. Biophys. Res. Commun.* **199,** 1209–1215
52. Luckman, S. P., Hughes, D. E., Coxon, F. P., Russell, R. G. R., and Rogers, M. J. (1998) *J. Bone Miner. Res.* **13,** 581–589
53. Yokoyama, K., Trobridge, P., Buckner, F. S., Scholten, J., Stuart, K. D., Van Voorhis, W. C., and Gelb, M. H. (1998) *Mol. Biochem. Parasitol.* **94,** 87–97
54. Ameisen, J. C., Idziorek, T., Billot-Mulot, O., Loyens, M., Tissier, J., Potentier, A., and Ouassi, A. (1995) *Cell Death Differ.* **2,** 285–300
55. Ylitalo, R., Mönkkönen, J., Urtti, A., and Ylitalo, P. (1996) *J. Lab. Clin. Med.* **127,** 200–206
56. Berenson, J. R., Rosen, L., Vescio, R., Lau, H. S., Woo, M., Sioufi, A., Kowalski, O., Knight, R. D., and Seaman, J. J. (1997) *J. Clin. Pharmacol.* **37,** 285–290